

# Circumstellar Shell Formation in Symbiotic Recurrent Novae

Kevin Moore<sup>1</sup> and Lars Bildsten<sup>1,2</sup>

## ABSTRACT

We present models of spherically symmetric recurrent nova shells interacting with circumstellar material in a symbiotic system composed of a red giant expelling a wind, and a white dwarf accreting from this material. Recurrent nova eruptions periodically eject material at high velocities ( $\gtrsim 10^3$  km/s) into the red giant wind profile, creating a decelerating shock wave as circumstellar material is swept up. High circumstellar material densities cause the shocked wind and ejecta to have very short cooling times of days to weeks. Thus, the late time evolution of the shell is determined by momentum conservation instead of energy conservation. We compute and show evolutionary tracks of shell deceleration, as well as post-shock structure. After sweeping up all the red giant wind, the shell coasts at a velocity  $\sim 100$  km/s, depending on system parameters. These velocities are similar to those measured in blue-shifted circumstellar material from the symbiotic nova RS Oph, as well as a few Type Ia supernovae that show evidence of circumstellar material, such as 2006X, 2007le, and PTF 11kx. Supernovae occurring in such systems may not show circumstellar material interaction until the inner nova shell gets hit by the supernova ejecta, days to months after the explosion.

*Subject headings:* binaries: symbiotic — circumstellar matter — novae, cataclysmic variables — shock waves — supernovae: general

## 1. Introduction

The range of Type Ia supernovae properties and new observations of these explosions at very early times (Nugent et al. 2011; Foley et al. 2012) points to a diversity of progenitor types. The long-standing view (see review by Hillebrandt & Niemeyer (2000)) has been that Type Ia result from a C/O white dwarf (WD) that has accreted enough material to compress the center to densities and temperatures so large that carbon fusion is ignited as an uncontrollable runaway that leads to an explosion. This requires the WD to nearly reach the Chandrasekhar mass ( $M_{\text{ch}}$ ), strongly constraining the binary evolution scenarios (Livio & Pringle 2011). The single degenerate (SD) scenario has a main sequence or slightly evolved donor, while the double degenerate (DD) scenario has another C/O WD as the donor - likely through a merger (Iben & Tutukov 1984; Webbink

---

<sup>1</sup>Department of Physics, Broida Hall, University of California, Santa Barbara, CA 93106, USA

<sup>2</sup>Kavli Institute for Theoretical Physics, Kohn Hall, University of California, Santa Barbara, CA 93106, USA

1984). These two channels may both occur, but a significant problem for the SD channel as a dominant mechanism is the lack of observed interaction between the supernova ejecta and the hydrogen expected to be present in such a system.

Recent observations have shed light on possible progenitors via evidence of interaction between the supernova ejecta and circumstellar material (CSM). Samples of SNe Ia show a bias towards blue shifted spectral features, such as Na absorption, which are likely outflows from the progenitor systems themselves (Sternberg et al. 2011). Previously reported Type Ias showing evidence of CSM include SNe 2002ic (Hamuy et al. 2003), 2005gj (Aldering et al. 2006), 2006X (Patat et al. 2007), 2007le (Simon et al. 2009), and PTF 11kx (Dilday et al., 2012). We note that there are alternative interpretations for 02ic as a Type Ic (Benetti et al. 2006) and 05gj as having an LBV progenitor (Trundle et al. 2008). Events such as SN 2006X and PTF 11kx show multiple blue shifted absorption features which may be interpreted as previously ejected material from successive recurrent nova outbursts in a symbiotic system such as RS Oph (Patat et al. 2007, 2011).

A nova is a thermonuclear runaway (TNR) of accreted hydrogen on a WD that ejects material from the WD’s hydrogen burning shell (Bode 2010). Simulations indicate that the TNR happens on a timescale ranging from days to years (Yaron et al. 2005), varying with the three main parameters of an accreting WD: the mass and temperature of the WD, along with the accretion rate onto the WD (Townesley & Bildsten 2004). Theoretical models also indicate that novae recur, with a recurrence time that is sensitive to the aforementioned parameters. Novae with more than one recorded outburst are said to be recurrent novae.

Recurrent novae can occur in both short period binaries and long period binaries (Anupama 2008). Short period binaries, such as T Pyx, can be cataclysmic variable (CV) systems ( $P_{\text{orb}} \sim 1$  hr) where a WD accretes matter from a star that overflows its Roche lobe. In long-period systems, such as RS Oph, the WD is in a wider binary ( $P_{\text{orb}} \sim 1$  yr) that is accreting from a wind ejected from the evolved donor, eg. a red giant. This type of nova is also referred to as a symbiotic recurrent nova (SyRNe). There are also symbiotic novae (SyNe) that have not been observed to recur (eg. AG Peg and RR Tel). Novae are uncommon among symbiotic systems: in  $\sim 200$  symbiotics known there are 9 SyNe and 4 SyRNe (Mikolajewska 2010). The accretion efficiencies are quite different between recurrent novae in short-period and long-period systems. In a short-period recurrent nova, there is little circumstellar material (CSM). In a symbiotic recurrent nova, the wind accretion efficiency is so low ( $\sim 1 - 10\%$ ) that most of the stellar wind is not accreted by the WD and remains as CSM.

SyRNe, especially RS Oph, have previously been investigated as possible SNe Ia progenitors (Hachisu & Kato 2001; Wood-Vasey & Sokoloski 2006; Hernanz & José 2008; Justham & Podsiadlowski 2008; Walder et al. 2010; Patat 2011). Detections of circumstellar material in RS Oph (O’Brien et al. 2006; Sokoloski et al. 2006), along with observations of spectral features blue-shifted by 30 – 50 km/s during outbursts (Iijima 2009; Patat et al. 2011) point to the existence of shells of material around the system with expansion velocities between the wind velocity,  $\approx 10 - 20$  km/s, and the ejecta velocity,  $\approx 3500$  km/s (Buil 2006; O’Brien et al. 2006).

In this paper, we examine the consequences of recurrent novae on the circumbinary environment. In §2 we show that the dense CSM in a symbiotic system leads to short radiative cooling times of the ejecta and shocked wind, making the kinematics of the nova shell determined by conservation of momentum. In §3, we derive the equations of motion for the spherically symmetric evolution of the nova shell and provide example realizations. The time-dependent post-shock structure of the decelerating ejecta and swept up wind is discussed in §4, along with possible instabilities in the ejecta and their effect on the long term evolution of nova shells. Finally, §5 discusses the implications of our model on potential supernovae in symbiotic systems.

## 2. Kinematics of the nova shell

An important difference between the evolution of nova ejecta in symbiotic systems versus those in cataclysmic variable systems is the large amount of CSM that the ejecta will interact with in a symbiotic system. The dense CSM around a symbiotic decelerates the nova ejecta and decreases the radiative cooling time by many orders of magnitude from the  $> 10^4$  years typical of nova shells interacting with the interstellar medium (Moore & Bildsten 2011). These short cooling times will cause momentum (rather than energy) conservation to determine the kinematics of the nova shell after a few weeks.

Although there is evidence that SyRNe such as RS Oph exhibit asymmetric mass ejection (O’Brien et al. 2006; Rupen et al. 2008), we consider a spherically symmetric model for simplicity. Between recurrent novae (with period  $t_{\text{rec}}$ ) the red giant (RG) donor is ejecting mass at a rate  $\dot{M}_w$  and velocity  $v_w$ , creating a density profile

$$\rho_w(r) = \frac{\dot{M}_w}{4\pi v_w r^2} = 2.2 \times 10^{-14} \text{ g cm}^{-3} \left( \frac{\dot{M}_w}{10^{-6} M_\odot/\text{yr}} \right) \left( \frac{v_w}{10 \text{ km/s}} \right)^{-1} \left( \frac{r}{1 \text{ AU}} \right)^{-2}, \quad (1)$$

out to a distance  $r_{\text{max}} = 6.3 \times 10^{14} \text{ cm} (v_w/10 \text{ km s}^{-1}) (t_{\text{rec}}/20 \text{ yr})$  immediately before the next nova. This density profile will be perturbed by the presence of the accreting WD as shown in the simulations by Walder et al. (2010), but remains nearly axisymmetric for slower wind velocities ( $v_w < 20 \text{ km/s}$ ). Each nova ejects a mass  $M_{\text{ej}}$ , which we scale as  $M_{\text{ej}} = f \dot{M}_w t_{\text{rec}}$  where  $f$  is a measure of both the accretion and explosion efficiency. We take  $f = 0.1$  as our fiducial, as various simulations show effective accretion rates between 10% and 2% of  $\dot{M}_w$  (Walder et al. 2008, 2010) with  $\sim 90\%$  of the accreted material being ejected during a nova for RS Oph-like systems (Hachisu & Kato 2001).

Our model for the evolution of the nova ejecta is motivated by observations and simulations of outbursts in RS Oph. Novae with short recurrence times also have short mass-ejection timescales (Yaron et al. 2005),  $\sim 1 - 5$  days, for recurrent novae such as RS Oph. Models of novae by Shen & Bildsten (2009) also show that short recurrence times require finely tuned mass-accretion rates. The mass-loss rate of the RG in RS Oph is  $\sim 10^{-6} M_\odot/\text{yr}$  (Rupen et al. 2008), which is consistent with a 20-year recurrence time given an accretion efficiency of  $f = 0.1$ . There are a range of

measurements of the ejecta mass itself. The ejecta mass of the 1985 outburst was measured to be  $\sim 10^{-6} M_{\odot}$  (O’Brien et al. 1992). Sokoloski et al. (2006) infer the ejecta mass of the 2006 outburst to be  $\sim 10^{-7} M_{\odot}$  due to the quick onset of a Sedov-Taylor phase, while Vaytet et al. (2011) estimate it as  $(2 - 5) \times 10^{-7} M_{\odot}$  from long-term simulations of the x-ray emission. Theoretical light curves of the 2006 nova by Hachisu et al. (2007) are best fit by an ejecta mass of  $(2 - 3) \times 10^{-6} M_{\odot}$ . The inferred ejecta mass in our model, neglecting the  $\sim 10\%$  of accreted material may remain on the WD (Hachisu & Kato 2001), is  $M_{\text{ej}} = f \dot{M}_w t_{\text{rec}} \approx 2 \times 10^{-6} M_{\odot}$ , on the high side of estimates for RS Oph. Most measurements of the ejecta velocity are  $v_{\text{ej}} = 3000 - 3500$  km/s (Hjellming et al. 1986; Buil 2006), but models from Vaytet et al. (2011) argue it is much higher, 6000 – 10000 km/s.

Early-time evolution of the ejection event is complex, requiring hydrodynamic wind-wind interactions (Vaytet et al. 2007, 2011), which we do not attempt to model. The 2006 outburst of RS Oph showed rapidly decelerating ejecta matching the self-similar Sedov-Taylor phase 3 – 10 days after the beginning of the outburst (Sokoloski et al. 2006; Bode et al. 2006), and quickly transitioning to the momentum-conserving phase after  $\sim 14$  days (Bode et al. 2006; Rupen et al. 2008). These observations indicate that the ejecta sweeps up enough mass in  $\sim 3$  days to get reverse-shocked and be in the self-similar phase. The cooling time of the postshock material is thus  $\sim 14$  days in order to make the transition to a momentum conserving phase.

The simplest model is to have the nova ejecta (here taken to be ejected all at once) coast into the  $\rho_w$  profile described above until it has swept up mass equal to itself, at at time  $t_{\text{sweep}} = 0.3$  days given our fiducials of  $\dot{M}_w = 10^{-6} M_{\odot}/\text{yr}$ ,  $v_w = 10$  km/s,  $v_{\text{ej}} = 3000$  km/s, and  $t_{\text{rec}} = 20$  yrs. A slightly more realistic model is to remove the core of the wind profile so the ejecta starts encountering mass after it has travelled roughly the orbital separation,  $a \sim 0.5$  AU. Doing so increases  $t_{\text{sweep}}$  to 3.0 days. After this time the shell is in the self-similar Sedov-Taylor phase until radiative cooling makes the energy-conserving assumption invalid.

While in the Sedov-Taylor phase, the position and velocity of the forward shock are given by (Chevalier 1982)

$$R_s = 9.8 \text{ AU} \left(\frac{f}{0.1}\right)^{1/3} \left(\frac{t_{\text{rec}}}{20 \text{ yrs}}\right)^{1/3} \left(\frac{v_w}{10 \text{ km/s}}\right)^{1/3} \left(\frac{v_{\text{ej}}}{3000 \text{ km/s}}\right)^{2/3} \left(\frac{t}{5 \text{ days}}\right)^{2/3} \quad (2)$$

$$v_s = 2300 \text{ km/s} \left(\frac{f}{0.1}\right)^{1/3} \left(\frac{t_{\text{rec}}}{20 \text{ yrs}}\right)^{1/3} \left(\frac{v_w}{10 \text{ km/s}}\right)^{1/3} \left(\frac{v_{\text{ej}}}{3000 \text{ km/s}}\right)^{2/3} \left(\frac{t}{5 \text{ days}}\right)^{-1/3}. \quad (3)$$

The post-shock material is assumed to be fully reverse-shocked in this phase, so we do not follow any transient reverse shocks. The immediate post-shock particle density at time  $t$  is given by the strong shock jump conditions (Draine 2011)

$$n_e = n_H = 9.1 \times 10^8 \text{ cm}^{-3} \left(\frac{\mu}{0.6}\right)^{-1} \left(\frac{f}{0.1}\right)^{-2/3} \left(\frac{\dot{M}_w}{10^{-6} M_{\odot}/\text{yr}}\right) \left(\frac{v_w}{10 \text{ km/s}}\right)^{-5/3} \left(\frac{v_{\text{ej}}}{3000 \text{ km/s}}\right)^{-4/3} \left(\frac{t_{\text{rec}}}{20 \text{ yrs}}\right)^{-2/3} \left(\frac{t}{5 \text{ days}}\right)^{-4/3}, \quad (4)$$

where  $\mu$  is the mean molecular weight of the material. The post-shock temperature is

$$T_s = 1.4 \times 10^7 \text{ K} \left( \frac{\mu}{0.6} \right) \left( \frac{v_s}{1000 \text{ km/s}} \right)^2. \quad (5)$$

The post-shock cooling is roughly isobaric (Bertschinger 1986) so the cooling time of the post-shock material is

$$t_{\text{cool}} = \frac{nkT_s}{(\gamma - 1)\Lambda}, \quad (6)$$

where  $\gamma = 5/3$  is the adiabatic index of the gas and  $\Lambda$  is the cooling function. Using the approximation for the cooling function of  $\Lambda/(n_e n_H) = 1.1 \times 10^{-22} T_6^{-0.7} \text{ erg cm}^3 \text{ s}^{-1}$  ( $T_6$  is the temperature in units of  $10^6 \text{ K}$ ), valid for  $10^5 \text{ K} < T < 10^{7.3} \text{ K}$  (Draine 2011), we calculate

$$t_{\text{cool}} = 36 \text{ days} \left( \frac{\mu}{0.6} \right)^{2.7} \left( \frac{f}{0.1} \right)^{1.8} \left( \frac{v_w}{10 \text{ km/s}} \right)^{2.8} \left( \frac{v_{\text{ej}}}{3000 \text{ km/s}} \right)^{3.6} \left( \frac{\dot{M}_w}{10^{-6} M_\odot/\text{yr}} \right)^{-1} \left( \frac{t_{\text{rec}}}{20 \text{ yrs}} \right)^{1.8} \left( \frac{t}{5 \text{ days}} \right)^{0.2}. \quad (7)$$

Using numerically computed cooling functions (Gnat & Sternberg 2007), rather than the power-law fit used above, reduces the cooling time to  $t_{\text{cool}} \approx t$  for the first 16 days of evolution, after which  $t_{\text{cool}} < t$ , roughly agreeing with the cooling time inferred from shock deceleration measurements of RS Oph outlined above.

### 3. Momentum-conserving evolution

We now derive the equation of motion for the momentum-conserving phase. As will be shown in §4, the rapid cooling of the shocked material at late times causes most of the ejecta to be moving at the same velocity as the shock front,  $v_s$ . The initial momentum of the system is split between the momentum in the ejecta,  $p_{\text{ej}} = f \dot{M}_w t_{\text{rec}} v_{\text{ej}}$  and that in the wind,  $p_w = (1 - f) \dot{M}_w t_{\text{rec}} v_w$ . We immediately derive the final coasting velocity of the shell after it has swept up all the wind, using  $p_{\text{final}} = \dot{M}_w t_{\text{rec}} v_{\text{coast}}$ , and thus

$$v_{\text{coast}} = f v_{\text{ej}} + (1 - f) v_w. \quad (8)$$

This implies coasting velocities of  $\simeq 100 \text{ km/s}$ , intermediate to both the wind and nova velocities. At a time  $t$  after the nova event the ejecta is sweeping up the wind, and the total wind mass swept up when the shell is at radius  $R_s(t)$ ,

$$M_{\text{sweep}}(t) = \int_{v_{\text{wind}} t}^{R_s(t)} 4\pi r^2 \rho_w(r) dr = \frac{\dot{M}_w}{v_w} (R_s(t) - v_w t). \quad (9)$$

The integration must start at  $v_{\text{wind}} t$  because that is the outer radius of the wind that was ejected since the nova outburst. From this, we define the column (number) density of the shell as

$$N = \frac{M_{\text{sweep}}(t)}{4\pi \mu m_p R_s(t)^2}. \quad (10)$$

The equation of motion for the shell arises from conservation of momentum:

$$(M_{\text{sweep}}(t) + f\dot{M}_w t_{\text{rec}})v_s(t) + \left[(1-f)\dot{M}_w t_{\text{rec}} - M_{\text{sweep}}(t)\right]v_w = \dot{M}_w t_{\text{rec}} [fv_{\text{ej}} + (1-f)v_w], \quad (11)$$

and thus

$$\ddot{R}_s = \frac{-(1-f)(v_s(t) - v_w)^2}{(1-f)(R_s(t) - v_w t) + f v_w t_{\text{rec}}}. \quad (12)$$

We give examples of  $R_s(t)$  and  $v_s(t)$  in Fig. 1.

We can also obtain a simpler equation of motion in the limit of negligible wind velocity ( $R_s \gg v_w t$ ),

$$R_s(t) = f v_w t_{\text{rec}} \left( \sqrt{1 + \frac{2v_{\text{ej}} t}{f v_w t_{\text{rec}}}} - 1 \right), \quad (13)$$

defining an evolution timescale

$$t_{\text{evol}} = \frac{f v_w t_{\text{rec}}}{2v_{\text{ej}}} = 4 \text{ days} \left( \frac{f}{0.1} \right) \left( \frac{v_w}{10 \text{ km/s}} \right) \left( \frac{t_{\text{rec}}}{20 \text{ yr}} \right) \left( \frac{v_{\text{ej}}}{1000 \text{ km/s}} \right). \quad (14)$$

Thus, for early times ( $t \ll t_{\text{evol}}$ )  $R_s(t) \propto t$ , while at late times  $R_s(t) \propto t^{1/2}$ . Coincidentally,  $t_{\text{evol}}$  is shorter than the mass-ejection timescale of the nova,  $t_{\text{ej}}$ , as well as  $t_{\text{cool}}$  in the Sedov-Taylor phase, and the momentum-conserving solution is not valid at these early times. Most of the observed shell evolution should therefore be in the  $R_s(t) \propto t^{1/2}$  phase. High resolution radio observations of the 2006 outburst of RS Oph tracked the deceleration of the shell, with Rupen et al. (2008) finding  $v_s \propto t^{-0.52}$  in the period 14 – 27 days after maximum - agreeing with the kinematics predicted by a momentum conserving phase after a brief Sedov-Taylor phase.

These calculations also yield the time required to completely sweep up the wind ejected since the previous nova,  $t_{\text{coast}}$ . From that time onward, the shell of material simply coasts outward at velocity  $v_{\text{coast}}$ . We show in the following section that the swept up material is in a geometrically thin shell at  $R_s$  and has a nearly uniform velocity throughout. In order to illustrate the resulting diversity in expected column densities,  $N_{\text{col}}$ , and coasting velocities, we rewrite our results in terms of ejecta energy,  $E_{\text{ej}}$  and  $\dot{M}_w$  since these are more accessible observationally. From  $E_{\text{ej}} = f\dot{M}_w t_{\text{rec}} v_{\text{ej}}^2/2$  we get

$$E_{\text{ej}} = \frac{\dot{M}_w t_{\text{rec}}}{2f} [v_{\text{coast}} - (1-f)v_w]^2. \quad (15)$$

From this, lines of constant  $v_{\text{coast}}$  are shown on the  $E_{\text{ej}} - \dot{M}_w$  plane in Figure 2. Typical ejecta energies of SyRNe are  $\sim 10^{42} - 10^{44}$  erg. The 1985 outburst of RS Oph had measured ejecta energies of  $8 \times 10^{42}$  erg (Bode & Kahn 1985) and  $1.1 \times 10^{43}$  erg (O’Brien et al. 1992), while the 2010 outburst of V407 Cyg was estimated at  $2 \times 10^{44}$  erg (Orlando & Drake 2012).

Nova recurrence times depend on the accretion rate and WD mass (Yaron et al. 2005; Shen & Bildsten 2009). Using the calculations from Shen & Bildsten (2009), we compute properties of the ejecta at the varying recurrence time as a function of accretion rate (for our purposes,  $\dot{M}_w$ ). We show the resulting timescales  $t_{\text{rec}}$  and  $t_{\text{coast}}$  in Figure 3. We are also interested in the state of the

nova ejecta when the next nova occurs. We plot the column density and the extent of the shell at  $t_{\text{rec}}$  in Figure 4. The value of  $N(t_{\text{rec}})$  for our fiducial values is  $4 \times 10^{19} \text{ cm}^{-2}$ .

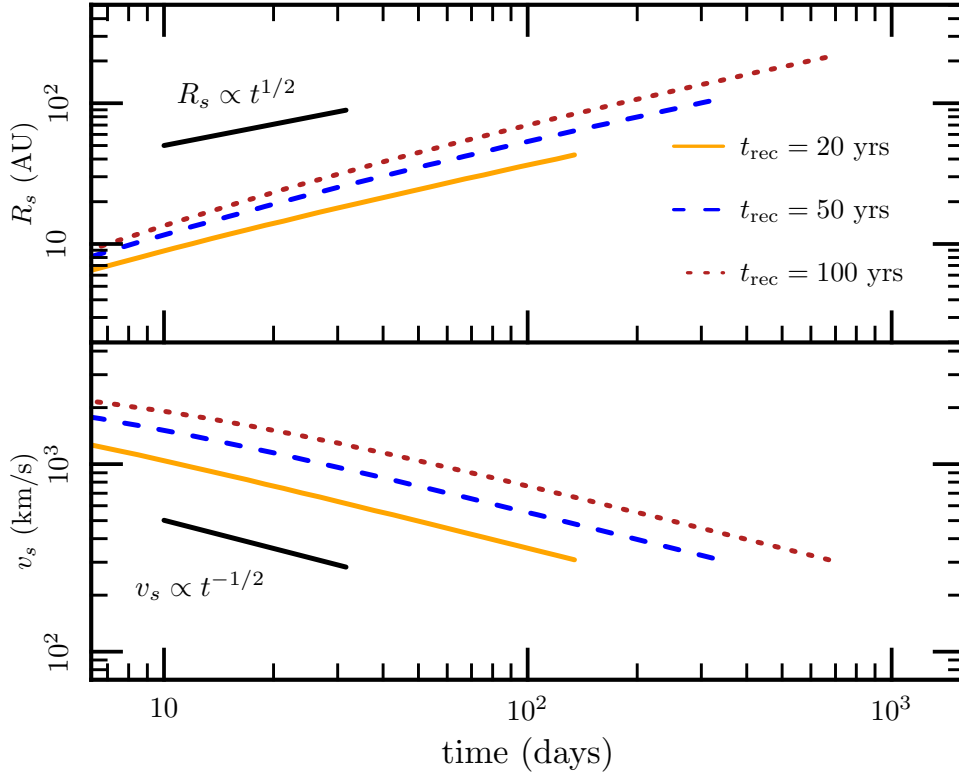


Fig. 1.— Shock radius ( $R_s$ , top panel) and velocity ( $v_s$ , bottom panel) as a function of time in the momentum conserving phase for different recurrence times. The lines end at  $t_{\text{sweep}}$ , once the ejecta has swept up all the wind, reaching a velocity  $v_{\text{coast}}$ . The accretion/explosion efficiency is  $f = 10^{-1}$ , the RG mass loss rate is  $\dot{M}_w = 10^{-6} M_{\odot}/\text{yr}$ , the wind velocity is  $v_w = 10$  km/s, and the ejecta velocity is  $v_{\text{ej}} = 3000$  km/s. This system has  $v_{\text{coast}} = 309$  km/s.



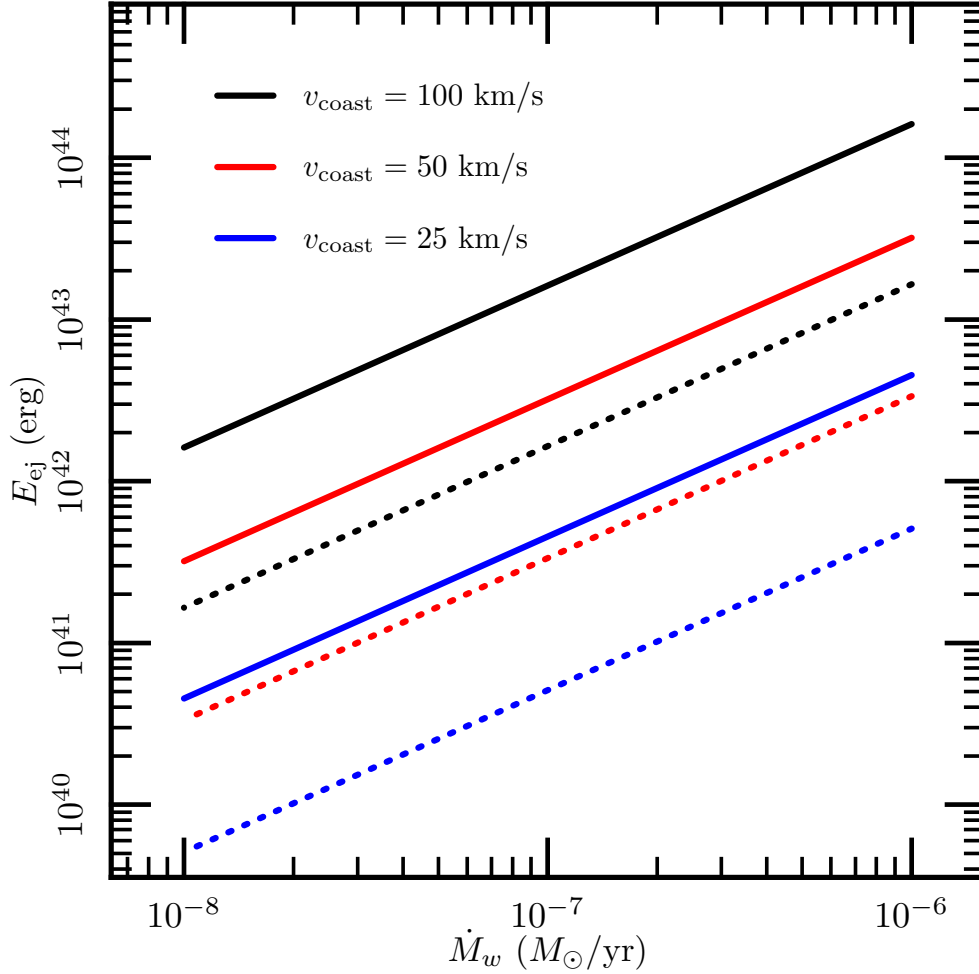


Fig. 2.— Lines of constant  $v_{\text{coast}}$  calculated on the  $\dot{M}_w - E_{\text{ej}}$  plane. The ejecta energy is assumed to be kinetic energy dominated:  $E_{\text{ej}} = f\dot{M}_w t_{\text{rec}} v_{\text{ej}}^2/2$ . Solid lines are for accretion/explosion efficiencies of  $f = 10^{-2}$  and dotted lines are for  $f = 10^{-1}$ . The other model parameters have been fixed at the fiducial values of  $v_w = 10 \text{ km/s}$  and  $t_{\text{rec}} = 20 \text{ yrs}$ .

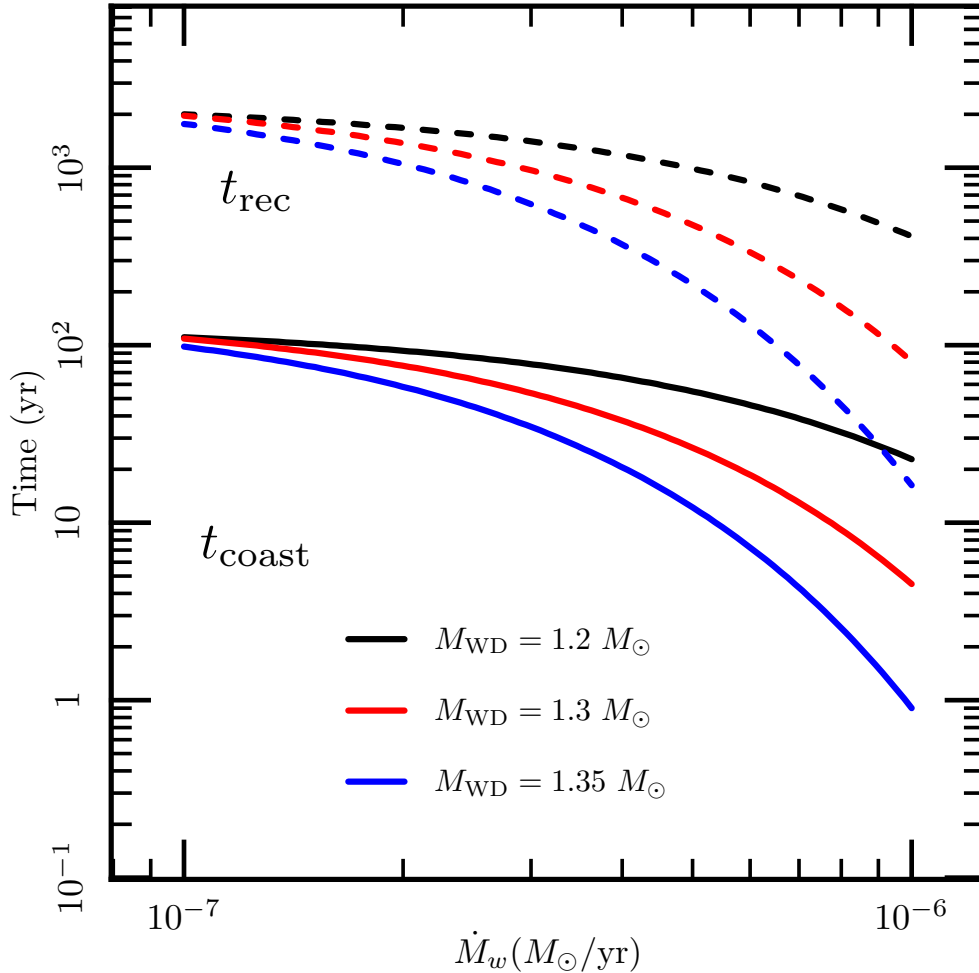


Fig. 3.— Variation of the recurrence time,  $t_{\text{rec}}$ , and the time to sweep up the entire wind,  $t_{\text{coast}}$ , with  $\dot{M}_w$  for novae on white dwarfs with different masses. The nova recurrence times vary with accretion rate and white dwarf mass as in Shen & Bildsten (2009). We calculate these curves with an accretion/explosion efficiency of  $f = 0.1$ , a wind velocity  $v_{\text{wind}} = 10$  km/s, and ejecta velocity  $v_{\text{ej}} = 5000$  km/s (thus a coasting velocity of  $v_{\text{coast}} = 509$  km/s). Since  $t_{\text{coast}}$  is always less than  $t_{\text{rec}}$ , the shell has reached its coasting velocity (i.e. the shock has broken out of the wind nebula) long before the next nova occurs.

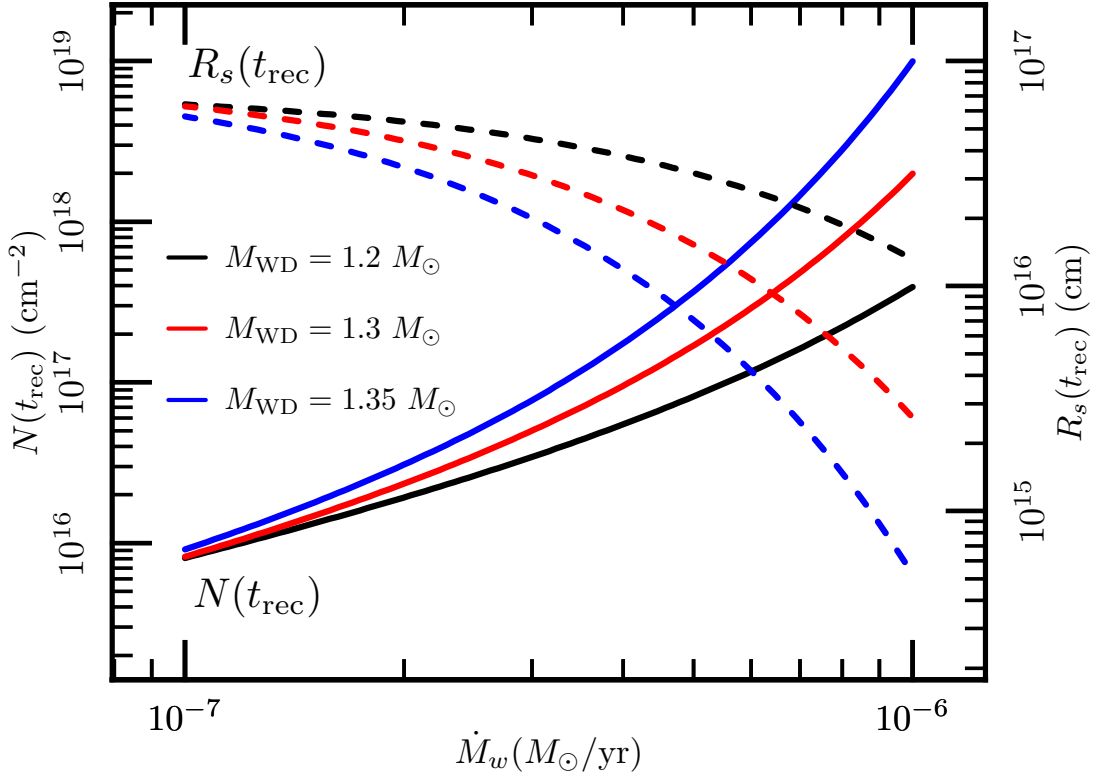


Fig. 4.— Lines of  $N(t_{\text{rec}})$  and  $R_s(t_{\text{rec}})$  for different WD masses as a function of  $\dot{M}_w$ . Solid lines are  $N(t_{\text{rec}})$  values (left axis), while dashed lines are  $R_s(t_{\text{rec}})$  values (right axis). The recurrence times vary with accretion rate and white dwarf mass as in Shen & Bildsten (2009). We calculate these curves with an accretion/explosion efficiency of  $f = 0.1$ , a wind velocity  $v_{\text{wind}} = 10$  km/s, and ejecta velocity  $v_{\text{ej}} = 3000$  km/s (thus a coasting velocity of  $v_{\text{coast}} = 309$  km/s).

#### 4. Post-shock structure and density estimates during deceleration

We have derived the expected column densities and coasting velocities from the simplest momentum conserving considerations. The resulting values agree with those inferred in the few clear observations of circumstellar shells (Dilday et al. 2012; Patat 2011; Patat et al. 2007; Hamuy et al. 2003). However, we have not calculated the thickness,  $\Delta R$ , of this shell, which sets the number density that is critical to photoionization and recombination calculations (Simon et al. 2009). Such estimates require a consideration of the post-shock structure in the deceleration phase.

##### 4.1. Cooling gas

Calculation of post-shock structure of the nova blast wave is divided into two main parts - cooling and cooled gas. Immediately behind the shock front is the region of active radiative cooling. Since we have already established that the cooling time is short ( $t_{\text{cool}} \ll R_s/v_s$ ), we calculate the fluid structure in this phase using the steady-state approximation. The hydrodynamic equations are written in Lagrangian coordinates and we work in spherical coordinates so that the radial fluid velocity is represented by the single variable  $u_r$ . In the steady state approximation we are left with the single independent variable  $r$ , indicating the radius from the explosion center. This yields three first-order differential equations:

$$\frac{\partial \rho}{\partial r} = \frac{-(\gamma - 1)\Lambda/u_r - 2\rho^2 u_r^2/r}{u_r^2 - \gamma P/\rho}, \quad (16)$$

$$\frac{\partial u_r}{\partial r} = -\frac{u_r}{\rho} \left( \frac{\partial \rho}{\partial r} \right) - \frac{2\rho u_r}{r}, \quad (17)$$

$$\frac{\partial T}{\partial r} = \frac{-(\partial P/\partial \rho)_T (\partial \rho/\partial r) - \rho u_r (\partial u_r/\partial r)}{(\partial P/\partial T)_\rho}. \quad (18)$$

The post-shock conditions at  $R_s$  come from the strong shock jump equations:  $\rho_1 = (\gamma + 1)\rho_w(R_s)/(\gamma - 1)$ ,  $kT_1 = 2(\gamma + 1)\mu m_p v_s^2/(\gamma + 1)$ , and the ideal gas equation of state  $P_1 = \rho_1 kT_1/(\mu m_p)$ . Here we use non-equilibrium cooling functions from Gnat & Sternberg (2007) since cooling can be rapid enough to throw ion abundances out of equilibrium. We integrate the fluid equations from  $R_s$  going in until the cooling rate drops off at  $T_c = 10^4$  K and radiative cooling is no longer important. The cooling time is always much less than the age of the shell, so the shocked wind also follows the momentum conserving evolution derived above. As the post-shock gas cools, it slows down relative to the shock front and increases in density.

We can estimate the density increase in the cold gas by noting that the cooling is roughly isobaric. The post-shock pressure is  $P_1 \approx \rho_0 v_s^2$ , which must equal the pressure of the gas after it has cooled,  $P_c = \rho_c kT_c/\mu m_p$  ( $c$  subscript indicates values in the cold gas). In terms of the thermal

velocity of the cold gas,  $v_{\text{th}} = \sqrt{3kT_c/\mu m_p} = 21$  km/s, this gives

$$\frac{\rho_c}{\rho_0} \approx \left(\frac{v_s}{v_{\text{th}}}\right)^2 = 20 \left(\frac{v_s}{100 \text{ km/s}}\right)^2. \quad (19)$$

Note the shock velocity is much slower than the ejecta velocity for all but the earliest evolutionary phases. A significant density increase in the cooled gas is also seen in Fig. 5 of Vaytet et al. (2011), although the simulation shown is at a much higher ejecta velocity ( $10^4$  km/s) and earlier time (3 days) so we can only make a qualitative comparison. From our derived density contrast, we can also estimate the thickness of the cold gas via  $4\pi R_s^2 \rho_c \Delta r \approx M_{\text{sweep}}(t)$  and thus

$$\frac{\Delta R}{R_s} \approx \left(\frac{v_{\text{th}}}{v_s}\right)^2. \quad (20)$$

The cold gas is therefore a thin, dense shell as compared to the post-shock gas at  $R_s$ .

## 4.2. Cold gas evolution

Behind the cooling layer is the layer of cold, swept up material. The evolution of this material depends on the secular evolution of the shock front, so the steady-state approximation breaks down. One method to obtain the structure in the swept up matter is to assume that the deceleration of the shock front is quickly transmitted to all the gas, so that the internal pressure gradient is determined by the evolution of the shock front,  $g \equiv dv_s/dt = -dP/\rho dr$ . By switching to mass coordinate behind the shock,  $m$ , we can write

$$\frac{dP}{dm} = \frac{g}{4\pi r^2}, \quad (21)$$

where  $m$  is the mass outside of radius  $r$ ,  $m = \int_r^{R_s} 4\pi r^2 \rho(r) dr$ , so  $m/M$  is a mass coordinate measured from inside the shock (so that the shock front is at  $m/M = 0$ ) and  $g$  is negative since the shell is decelerating. The entropy of each mass element of wind gets frozen after radiative cooling has ceased. We find the entropy structure,  $S(m)$ , by using the steady state cooling calculation described in the previous section. Finally, we assume that most of the mass is concentrated in a thin shell near the shock front ( $r = R_s$ ), and calculate the pressure structure from hydrostatic balance,

$$\int_{P(0)}^{P(m)} dP = g \int_0^m \frac{dm}{4\pi r^2} \quad (22)$$

$$\Rightarrow P(m) = P(0) + \frac{gM}{4\pi R_s^2} \left(\frac{m}{M}\right). \quad (23)$$

Combining this with the input entropy profile and the adiabatic relations  $\rho \propto (P/P_0)^{3/5}$  and  $T \propto (P/P_0)^{2/3}$  gives us the full post-shock structure (except for the velocity), shown in blue lines

in Fig. 5. We compare this calculation to that in Bertschinger (1986) which assumes a self-similar solution in the cold-gas. That solution does not reproduce the post-cooling entropy of the shocked wind at early times because it uses a single power-law evolution in time, while the solution is transitioning from a radiative shock to a momentum-conserving one. The thin-shell approximation is more accurate for the regime where the outward moving shock has not yet reached  $R_s \propto t^{1/2}$ .

### 4.3. Instabilities and long-term evolution

Chevalier & Imamura (1982) investigated instabilities of radiative shock waves in the ISM. Their analysis showed that for a cooling function  $\Lambda \propto T^\alpha$ , oscillatory cooling instabilities appear for  $\alpha < 0.4$  (fundamental mode) and  $\alpha < 0.8$  (first overtone). Recall that a fit to the equilibrium cooling function at relevant temperatures had  $\Lambda \propto T^{-0.7}$ , indicating an instability. We note, as do Chevalier & Imamura (1982), that non-equilibrium effects significantly alter the cooling function (Gnat & Sternberg 2007) so a true time-dependent calculation is necessary to determine the presence of instabilities in such radiative shocks. Such time-dependent calculations have been carried out for 1D piston-driven radiative shocks (Innes et al. 1987; Gaetz et al. 1988), showing that shock velocities above  $v_s \approx 150$  km/s are ‘overstable’, having oscillations in shock position relative to the piston location. Thus, steady-state shock calculations are not suitable for investigating the luminosities and spectra during the cooling phase of a radiative shock in our model.

## 5. Supernovae in symbiotic systems

Supernovae occurring in such systems should show signals of interaction with CSM. Donor star mass loss rates in symbiotic systems vary between first-ascent RGB stars,  $10^{-7} - 10^{-5} M_\odot/\text{yr}$  (Seaquist & Taylor 1990), and extreme asymptotic giant branch (AGB) stars. The SNe Ia that have shown prominent interaction with CSM vary in strength from SN 2005gj (Aldering et al. 2006) to SN 2002ic (Wood-Vasey & Sokoloski 2006; Nomoto et al. 2005; Hamuy et al. 2003) to PTF 11kx (Dilday et al. 2012), implying a continuum of progenitor properties such as CSM mass accumulation or time since the most recent nova event. The prominent interaction seen in these SNe Ia appear to require a mass of CSM greater than can be provided by an RGB wind on the time-scale of 100 years (suggesting a recent AGB phase), but less prominent interaction with the wind/ nova shells of an RGB star is also detectable.

Assuming a supernova could go off at any phase within the recurrent nova cycle, there will likely be some CSM inside the inner nova cavity that the supernova will quickly sweep up. Early-time radio observations have looked for CSM interactions in Type Ia’s assuming companion wind (Panagia et al. 2006), and placed stringent mass loss rates ( $\dot{M}_w \lesssim 3 \times 10^{-8} M_\odot/\text{yr}$ ) on winds in the progenitor systems assuming uniform progenitors across a set of Ia’s. Individual Ia’s used in that study had typical mass-loss constraints  $\dot{M}_w \lesssim 10^{-7} - 10^{-6} M_\odot/\text{yr}$ . Recently, the excellent

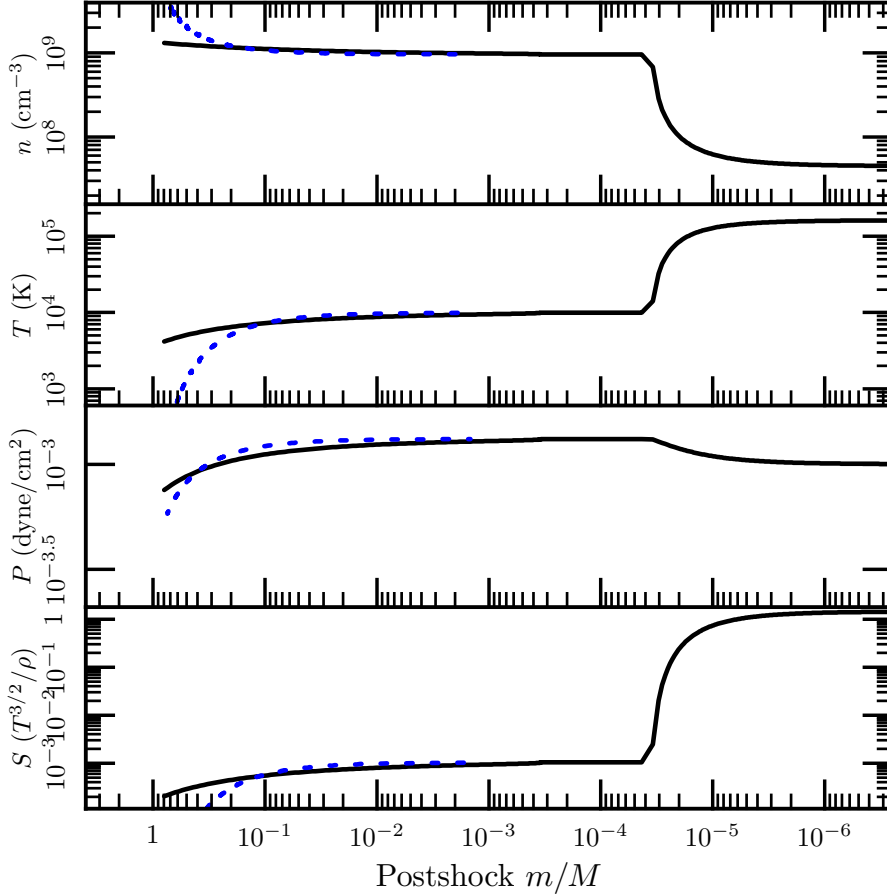


Fig. 5.— Number density, pressure, temperature, and entropy (via  $T^{3/2}/\rho$ ) evolution versus mass coordinate behind the shock. The black lines are from a calculation using the separation of variable method following Bertschinger (1986), while the blue dashed lines are from the thin-shell calculation described in this paper. Gas is cooling from the shock front until  $m/M \approx 4 \times 10^{-5}$ , while gas behind that has already cooled (from a slightly different shock temperature). The gas near the rear of the shell is at an even lower temperature since it has undergone significant adiabatic expansion. These structure plots show when a nova shell has just swept up all the wind (at  $t_{\text{coast}} = 1.1$  yrs) in a system with  $f = 0.1$ ,  $v_{\text{ej}} = 1000$  km/s,  $\dot{M}_w = 10^{-6} M_{\odot}/\text{yr}$ ,  $v_w = 10$  km/s, and  $t_{\text{rec}} = 20$  yrs.

early-time observations of 2011fe indicate  $\dot{M}_w \lesssim 6 \times 10^{-10} M_\odot/\text{yr}$  for that system (Chomiuk et al. 2012).

As pointed out in Wood-Vasey & Sokoloski (2006), these early time CSM interactions could be avoided if a previous nova swept out a cavity that has been refilled for less than  $t_{\text{rec}}$ . Assuming an ejecta velocity of  $v_{\text{SN}} = 10^4 \text{ km/s}$  for the supernova, then in the first  $t$  days it could sweep up a wind mass that had been ejected for the last  $t_{\text{SN}}$  years, where

$$t_{\text{SN}} = 5.5 \text{ yrs} \left( \frac{v_{\text{SN}}}{10^4 \text{ km/s}} \right) \left( \frac{v_w}{10 \text{ km/s}} \right)^{-1} \left( \frac{t}{2 \text{ days}} \right). \quad (24)$$

Thus  $t_{\text{SN}}$  is on the order of the recurrence times for very high mass WDs (Yaron et al. 2005; Shen & Bildsten 2009), so even supernovae with exceptionally early radio observations such as SN 2011fe could hide significant CSM if it were in a SyRNe system. Of course, there are many other lines of evidence that rule out such a progenitor for SN 2011fe (Bloom et al. 2012; Chomiuk et al. 2012; Horesh et al. 2012; Margutti et al. 2012; Nugent et al. 2011; Li et al. 2011).

From Figure 4, the location of the nova shell at  $t_{\text{rec}}$  gives an upper limit on the timescale of interaction with the innermost nova shell of

$$t_{\text{inner}} = 12 \text{ days} \left( \frac{R_s}{10^{15} \text{ cm}} \right) \left( \frac{v_{\text{SN}}}{10^4 \text{ km/s}} \right)^{-1}. \quad (25)$$

This timescale can vary greatly due to the variability in  $R_s$ , and we note it is consistent with the 22 day and 60 day brightenings observed in the light curve of SN 2002ic (Hamuy et al. 2003; Wood-Vasey & Sokoloski 2006).

## 6. Conclusions

The origins of Type Ia supernovae continue to be debated, with some showing evidence of a single-degenerate progenitor (Dilday et al. 2012; Simon et al. 2009; Patat et al. 2007), and others with strong evidence of a double-degenerate progenitor (Bloom et al. 2012; Chomiuk et al. 2012; Horesh et al. 2012; Margutti et al. 2012; Nugent et al. 2011; Li et al. 2011). There is thus mounting evidence of multiple channels to a Type Ia.

Decelerating nova shells in SyRNe can have velocities consistent with the few SNe Ia with CSM detections. Nova shells are thin and have high density contrasts ( $\sim 100\times$ ) compared to the ambient medium, which are important for calculating atomic populations. Additional work on simulating the ionization states of these shells and subsequent radiative transfer during a supernovae is necessary in order to make detailed comparisons to specific spectra. Supernovae in SyRNe systems could be detected both via time-dependent absorption lines in previous shells, and via rebrightening of the light curve as supernova ejecta hits the shells.

We note some shortcomings of this model for interacting Type Ia's. Firstly, novae (and RS Oph in particular) are known to have asymmetric ejecta (Hjellming et al. 1986; O'Brien et al. 2006;



Rupen et al. 2008), which is not accounted for in our model. An asymmetric outburst (and/or wind profile) can change the ratio of momentum in the wind to that in the ejecta, and thus the coasting velocities. The general picture of a decelerating shell governed by momentum conservation remains, with details such as the density contrast and coasting velocity depending on orientation.

We thank Ben Dilday, Andy Howell, Sterl Phinney, and Jenő Sokoloski for useful discussions and clarifications. This work was supported by the National Science Foundation under grants PHY 11-25915 and AST 11-09174.

## REFERENCES

- Aldering, G., et al. 2006, *ApJ*, 650, 510
- Anupama, G. C. 2008, in *Astronomical Society of the Pacific Conference Series*, Vol. 401, RS Ophiuchi (2006) and the Recurrent Nova Phenomenon, ed. A. Evans, M. F. Bode, T. J. O’Brien, & M. J. Darnley, 31
- Benetti, S., Cappellaro, E., Turatto, M., Taubenberger, S., Harutyunyan, A., & Valenti, S. 2006, *ApJ*, 653, L129
- Bertschinger, E. 1986, *ApJ*, 304, 154
- Bloom, J. S., et al. 2012, *ApJ*, 744, L17
- Bode, M. F. 2010, *Astronomische Nachrichten*, 331, 160
- Bode, M. F., & Kahn, F. D. 1985, *MNRAS*, 217, 205
- Bode, M. F., et al. 2006, *ApJ*, 652, 629
- Buil, C. 2006, *Central Bureau Electronic Telegrams*, 403, 1
- Chevalier, R. A. 1982, *ApJ*, 258, 790
- Chevalier, R. A., & Imamura, J. N. 1982, *ApJ*, 261, 543
- Chomiuk, L., et al. 2012, *ApJ*, 750, 164
- Dilday, B., et al. 2012, *ArXiv e-prints*
- Draine, B. T. 2011, *Physics of the Interstellar and Intergalactic Medium*, ed. Draine, B. T.
- Foley, R. J., et al. 2012, *ApJ*, 744, 38
- Gaetz, T. J., Edgar, R. J., & Chevalier, R. A. 1988, *ApJ*, 329, 927
- Gnat, O., & Sternberg, A. 2007, *ApJS*, 168, 213

- Hachisu, I., & Kato, M. 2001, *ApJ*, 558, 323
- Hachisu, I., Kato, M., & Luna, G. J. M. 2007, *ApJ*, 659, L153
- Hamuy, M., et al. 2003, *Nature*, 424, 651
- Hernanz, M., & José, J. 2008, *New A Rev.*, 52, 386
- Hillebrandt, W., & Niemeyer, J. C. 2000, *ARA&A*, 38, 191
- Hjellming, R. M., van Gorkom, J. H., Seaquist, E. R., Taylor, A. R., Padin, S., Davis, R. J., & Bode, M. F. 1986, *ApJ*, 305, L71
- Horesh, A., et al. 2012, *ApJ*, 746, 21
- Iben, Jr., I., & Tutukov, A. V. 1984, *ApJS*, 54, 335
- Iijima, T. 2009, *A&A*, 505, 287
- Innes, D. E., Giddings, J. R., & Falle, S. A. E. G. 1987, *MNRAS*, 226, 67
- Justham, S., & Podsiadlowski, P. 2008, in *Astronomical Society of the Pacific Conference Series*, Vol. 401, RS Ophiuchi (2006) and the Recurrent Nova Phenomenon, ed. A. Evans, M. F. Bode, T. J. O'Brien, & M. J. Darnley, 161
- Li, W., et al. 2011, *Nature*, 480, 348
- Livio, M., & Pringle, J. E. 2011, *ApJ*, 740, L18
- Margutti, R., et al. 2012, *ApJ*, 751, 134
- Mikolajewska, J. 2010, *ArXiv e-prints*
- Moore, K., & Bildsten, L. 2011, *ApJ*, 728, 81
- Nomoto, K., Suzuki, T., Deng, J., Uenishi, T., & Hachisu, I. 2005, in *Astronomical Society of the Pacific Conference Series*, Vol. 342, 1604-2004: Supernovae as Cosmological Lighthouses, ed. M. Turatto, S. Benetti, L. Zampieri, & W. Shea, 105
- Nugent, P. E., et al. 2011, *Nature*, 480, 344
- O'Brien, T. J., Bode, M. F., & Kahn, F. D. 1992, *MNRAS*, 255, 683
- O'Brien, T. J., et al. 2006, *Nature*, 442, 279
- Orlando, S., & Drake, J. J. 2012, *MNRAS*, 419, 2329
- Panagia, N., Van Dyk, S. D., Weiler, K. W., Sramek, R. A., Stockdale, C. J., & Murata, K. P. 2006, *ApJ*, 646, 369

- Patat, F. 2011, ArXiv e-prints
- Patat, F., Chugai, N. N., Podsiadlowski, P., Mason, E., Melo, C., & Pasquini, L. 2011, *A&A*, 530, A63
- Patat, F., et al. 2007, *Science*, 317, 924
- Rupen, M. P., Mioduszewski, A. J., & Sokoloski, J. L. 2008, *ApJ*, 688, 559
- Seaquist, E. R., & Taylor, A. R. 1990, *ApJ*, 349, 313
- Shen, K. J., & Bildsten, L. 2009, *ApJ*, 692, 324
- Simon, J. D., et al. 2009, *ApJ*, 702, 1157
- Sokoloski, J. L., Luna, G. J. M., Mukai, K., & Kenyon, S. J. 2006, *Nature*, 442, 276
- Sternberg, A., et al. 2011, *Science*, 333, 856
- Townsley, D. M., & Bildsten, L. 2004, *ApJ*, 600, 390
- Trundle, C., Kotak, R., Vink, J. S., & Meikle, W. P. S. 2008, *A&A*, 483, L47
- Vaytet, N. M. H., O’Brien, T. J., & Bode, M. F. 2007, *ApJ*, 665, 654
- Vaytet, N. M. H., O’Brien, T. J., Page, K. L., Bode, M. F., Lloyd, M., & Beardmore, A. P. 2011, *ApJ*, 740, 5
- Walder, R., Folini, D., Favre, J. M., & Shore, S. N. 2010, in *Astronomical Society of the Pacific Conference Series*, Vol. 429, *Numerical Modeling of Space Plasma Flows*, Astronom-2009, ed. N. V. Pogorelov, E. Audit, & G. P. Zank, 173
- Walder, R., Folini, D., & Shore, S. N. 2008, *A&A*, 484, L9
- Webbink, R. F. 1984, *ApJ*, 277, 355
- Wood-Vasey, W. M., & Sokoloski, J. L. 2006, *ApJ*, 645, L53
- Yaron, O., Prialnik, D., Shara, M. M., & Kovetz, A. 2005, *ApJ*, 623, 398